Silicon (2023) 15:4259–4275
https://doi.org/10.1007/s12633-023-02347-0

ORIGINAL PAPER

Mechanical Characteristics and Wear Behaviour of Al/SiC and Al/SiC/B_4C Hybrid Metal Matrix Composites Fabricated Through Powder Metallurgy Route

P. Bharathi[1] · T. Sampath kumar[1]

Received: 11 January 2023 / Accepted: 10 February 2023 / Published online: 22 February 2023

Abstract
In the present study aluminium metal matrix composites (Al-MMCs) reinforced with different Wt% (2,3,4,5 and 6) of Silicon carbide (SiC) and hybrid composites of aluminium matrix reinforced with different Wt% (2,3,4,5 and 6) of SiC and constantly adding Boron carbide (B_4C) with 2 wt% were fabricated using a cost effective powder metallurgy (PM) method and the mechanical alloying process. Mechanical properties like micro structure, phase analysis, hardness, compression strength, density, porosity and wear were characterized and investigated for the aluminium matrix composite (AMC) samples. Microstructural characterization of sintered samples was performed using a Scanning electron microscope with energy dispersive X-ray analysis. XRD analysis confirmed the peak identification of Aluminium, SiC and B_4C particulates in the (Al-MMCs) composites. The hardness values of the composites Al+6wt% SiC and Al+4wt%SiC+2wt%B_4C were seen as 20.6% higher than those of pure aluminium matrix. Increase in the hardness of the composite was seen due to grain refinement and resistance to dislocation motion. The existence of SiC particles in Al matrix was seen having the ability to improve the hardness value of the composites. The addition of SiC and B_4C reinforcements in the Al matrix alloy has the potential to greatly increase the compressive strength of the AMCs. The density of hybrid composites was seen having a major impact on the influence of SiC and B_4C particulates. The wear resistance of the hybrid composites were examined under load range of 5 and 10 N, with sliding speed of 0.1 m/s. The synergistic effect of reinforcing particles was seen as assisting the improvement of wear resistance due to the relative concentration of SiC and B_4C. The incorporation of SiC and B_4C reinforcements into the Aluminium matrix hybrid composite can substantially increase the hardness, compressive strength, and wear resistance of the composites.

Keywords Metal matrix composites · Silicon carbide · Boron carbide · Powder metallurgy · Hardness · SEM · XRD · Density

1 Introduction

Metal matrix composite (MMCs) find extensive use in the automobile industry due to their high performance with lightweight, lesser density, greater strength and cheaper cost [1]. In general, MMC is typically made of Aluminium, Magnesium, Titanium, Copper and other metal [2]. Aluminium metal composites (AMCs) provide useful lightweight material of a basic class that can be used in the manufacture of a variety of different components such as pistons, cylinders, engine blocks etc. [3, 4]. Addition of various reinforcements can be made to the matrix material for making the composite much stronger. AMCs have improved mechanical properties such as high elastic modulus, greater hardness, and high tensile strength at elevated temperatures, as well as significant weight reduction compared to unreinforced alloys [5–7]. Ceramic materials such as Al_2O_3, SiC, and B_4C are commonly found in automobile applications and aerospace components due to their enhanced hardness, strength and corrosion resistance [8]. The chemical compatibility of SiC with aluminium is also excellent, as it forms an adequate bond with the matrix without the formation of any intermetallic

✉ T. Sampath kumar
sampathtpp@gmail.com

P. Bharathi
bharathi.p2019@vitstudent.ac.in

[1] School of Mechanical Engineering, Vellore Institute of Technology, Vellore 632014, Tamil Nadu, India

phase [9]. The superior hardness, low density and impressive thermal and chemical durability of boron carbide particles make them a promising reinforcement among ceramic materials. The addition of a metal phase to boron carbide can help significant improvement in its mechanical properties and elimination of its processing problems [10]. Powder metallurgy is a frequently used approach for the manufacture of composites, compared to the infiltration method and the stir casting process. It is the most extensively used technology due to its ability to convert any powder into a finished product. It is an alternative technique for the manufacture of MMCs in new of their low starting price, better quality, reduced material waste and capability to create complicated components economically. Powder metallurgy has witnessed utilizations in various fields such as automotive, defence, aerospace etc. [11]. It is a very efficient method used in the recycling of metals and alloy recycling. The process provides almost a net-shaped product with no need for additional machining, otherwise small machining is required. In powder metallurgy, the material is treated below its melting point [12–14]. When compared with the single reinforcement in metal matrix composites, hybrid composites are able to achieve superior mechanical properties due to different reinforcement properties. In order to achieve superior mechanical properties, hybrid metal matrix composites are utilized with various types of reinforcement in a variety of sizes, shapes, and wt%. Cao Fenghong et al. (2018) investigated the ability of the presence of stronger reinforcement like SiC (5, 7.5, 10Wt%) and WC (5, 7.5, 10wt%) in the aluminium matrix alloy for a substantial enhancement of the hardness of hybrid composites compared to monolithic alloys. Aluminium matrix alloy reinforced with 10wt% of SiC and 10wt% of WC obtained a high hardness of 98.54 HV with improved metallurgical properties [15]. Habibur Rahman et al. (2014) observed improvement in the hardness and tensile strength of the composites with the addition of SiC to the Al matrix [16]. Gutema endalkachew mossia et al. [17] (2017) did work on an Al–Mg-Si hybrid composite fabricated through powder metallurgy, which enhanced the mechanical properties. A substrate influence from the effect of volume fraction of SiC-Mg particulates was seen in the hardness and density of the composites. SiC (12–16 Wt%) and Mg (1–1.5 Wt%) in optimum content was added to the aluminium matrix, which revealed superior mechanical properties. An increase in the hardness (76.5 HBR) and porosity (80%) of the composite was seen following an increase in reinforcement wt%. Jianhua Liu et al. [18] (2020) prepared aluminium metal matrix reinforced SiC composites by microwave sintering. According to the ideal condition, Al/15 vol% SiC composites were seen having a relative density of 96.14% and a hardness of 130 HV. A comprehensive literature review indicates the addition of reinforcement to the aluminium matrix causing an increase in mechanical and physical characteristics. Carbides, Oxides and certain intermetallic compounds find extensive use in Al-MMCs as reinforcing materials. According to the previous research, it is abundantly clear that a great number of researchers have conducted work to study the microstructural, mechanical, and wear behaviour of Al/SiC composites by varying the weight/volume fraction of SiC using powder metallurgy. However, only a few studies are seen in the determination of the effect of powder metallurgy on hybrid Al- composites reinforced with SiC and B_4C. Due to the higher cost of B_4C powders, there was only a small amount of research done on B_4C reinforced aluminium matrix composites. However, B_4C is a desirable reinforcement material not only because of its superior chemical and thermal stability, but also because of its lower density, higher hardness, and superior bonding property. The novel aspect of this study was the production of aluminium hybrid composite through the use of powder metallurgy process, which involved the addition of a low reinforcement wt% of SiC and B_4C particles in order to achieve high mechanical properties. The objective of this study is to investigate the effect, that the amount of reinforcement has influenced the changes in microstructural and mechanical properties of Al+SiC and Al+SiC+B_4C composites that are produced using the powder metallurgy technique. Non-reinforced pure aluminium samples were fabricated for a comparative study. Mechanical characteristics such as SEM, XRD, Hardness, Compression, Wear, Density, and Porosity were analyzed and reported for Al+SiC and Al+SiC+B_4C composites.

2 Experimental Investigation

The aluminium metal matrix (99.0% purity) powder and the ceramic powders of SiC and B_4C were purchased from Pallav Chemicals and solvents Pvt Ltd in Mumbai, India. SiC and B_4C powders (99.5% purity) with particle size less than 50 microns were used as reinforcements. Powder characteristics of Al, SiC & B_4C are shown in Table 1. Figure 1(a) represents the morphological image of as-received aluminium powder and particle size distribution of Al powder. The morphology image of SiC and particle size distribution of SiC particles are shown in Fig. 1(b) and the morphology image of B_4C and particle size distribution of B_4C particles

Table 1 Powder characteristics of Al, SiC and B_4C particles

Characteristics	Aluminium	Silicon carbide	Boron Carbide
Density (g/cm^3)	2.7	3.21	2.52
Melting Point (^{o}C)	660.37	2730	2350
Mesh Size	325	400	220
Morphology	Irregular	Angular	Angular

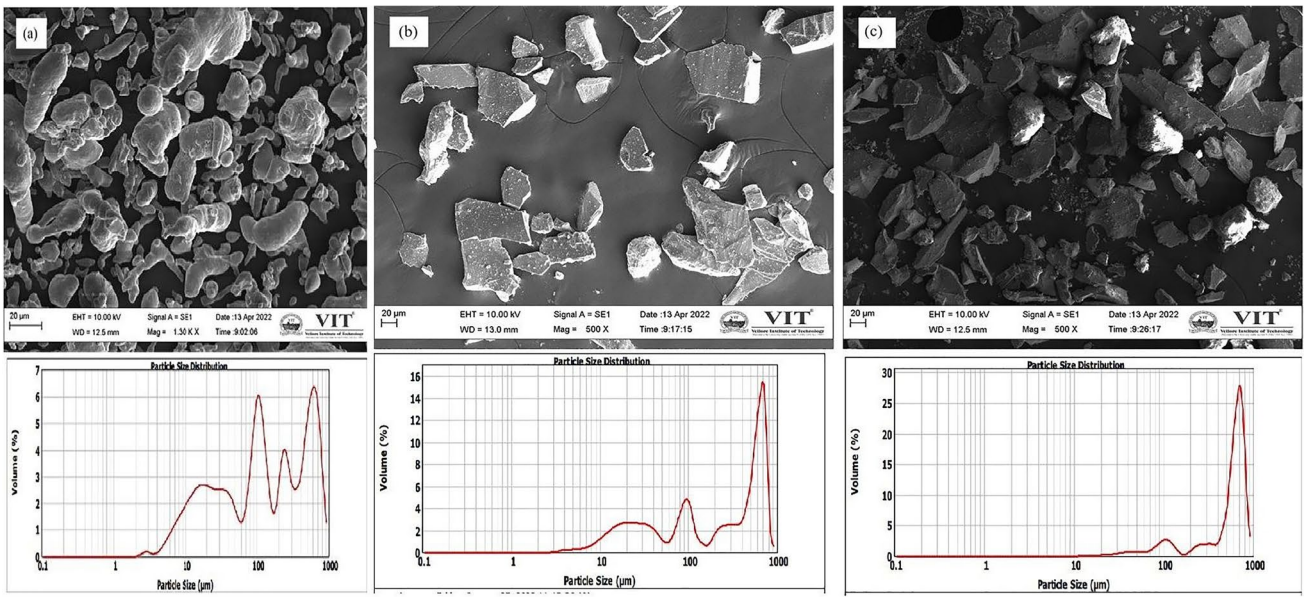

Fig. 1 Powder particle morphology and particle size distribution of **a**) Aluminium, **b**) Silicon carbide and **c**) Boron carbide

Table 2 Characteristic values for the particle size distribution of different powders

Powder name	d_{10} (µm)	d_{50} (µm)	d_{90} (µm)	Span	Specific Surface Area (m^2/g)
Aluminium	13.040	116.750	644.150	5.406	0.158
SiC	17.223	272.510	717.556	2.570	0.115
B_4C	108.140	628.017	791.325	1.088	0.221

are shown in Fig. 1(c). Characteristic values for the particle size distribution of powders are shown in Table 2. Details of the chemical composition of the aluminium matrix are shown in Table 3. A Precision weight scale (Mettler Toledo) was used in the calculation of the weights (2 to 6 Wt%) of reinforcements. Simultaneously matrix and reinforcements were thoroughly blended by mechanical stirring at 2000 rpm for obtaining a homogenous powder mixture. Following the completion of the blending process, the compacting die was preheated to 350 °C for the removal of the moisture content and a reduction in the formation of air bubbles during the mixing of the matrix and reinforcements. Reinforcement particles were preheated to 250 °C for the removal of the moisture present in the reinforcements and improvement of wettability. This study was carried out with three distinct powder metallurgy processes, namely (i) Blending (ii) Compacting and (iii) Sintering. The composites were fabricated by using aluminium matrix material with SiC (2 to 6 Wt%), and B_4C (2 wt.%) as reinforcements. Compacting was done using a hydraulic jack with high pressure of 735Mpa for the preparation of the sample size of 26 mm in diameter and 25 mm in height. Following compacting, the material was degassed at 400 °C for 3 h for the removal of moisture, hydrogen and oxygen. Finally, the samples obtained were sintered in a high-temperature furnace with an operating temperature of 550 °C for 3 h. Following sintering, the composites were allowed for furnace cooling. Following the fabrication process, the samples were characterized for microstructure analysis. The sintered composites of Al+SiC and Al+SiC+B_4C are shown in Fig. 2(a) and (b) respectively. Figure 3(a) shows the microstructure of the aluminium matrix and Fig. 3(b) Elemental composition analysis of the aluminium matrix was assessed by energy dispersive spectroscopy. Figure 3(c) represents the microstructure of Al+SiC composite and Fig. 3(d) shows the elemental composition analysis of the Al+SiC composite. Figure 3(e) shows the microstructure of the Al+SiC+B_4C composite and Fig. 3(f) shows the Elemental composition analysis of the Al+SiC+B_4C composite. An optical microscope (Olympus, metallurgical microscope) and a Scanning electron microscope (Carl ZEISS EVO18) were used in the analysis of the microstructural characteristics of the

Table 3 Chemical composition of Aluminium powder

Elements	Al	Si	Cu	Fe	Mn	Ti
Composition (%)	Balance	0.1	0.02	0.1	0.02	0.03

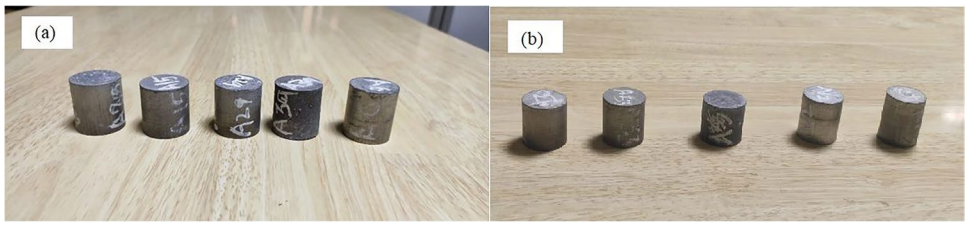

Fig. 2 Sintered composite samples (**a**) Al+SiC (**b**) Al+SiC+B_4C

composites. Analysis of phase identification for composites was done with the help of X-ray diffraction analysis (Bruker D8 diffractometer). Sintered composite hardness was calculated using a Vickers hardness testing machine (Model: Matsuzawa (MMT-x) with a force of 100 gf dwell sec as 10 s) with ASTM E-384 standard. The mean hardness of each composite was determined using ten measurements obtained in different locations. Compression tests were carried out at room temperature using a universal testing machine (Instron 8801), and they were performed in accordance with the ASTM E9 standard. The length of each specimen was 16 mm, the diameter was 8 mm, and the length-to-diameter ratio was 2.0. Theoretical density calculation of the composites was performed according to the ASTM B962-15 using the mixture rule. The experimental density of the composites was calculated using the Archimedes principle with the help of Mettler Toledo equipment. For the wear test, a pin-on-disc testing machine with the model number DUCOM TR-201

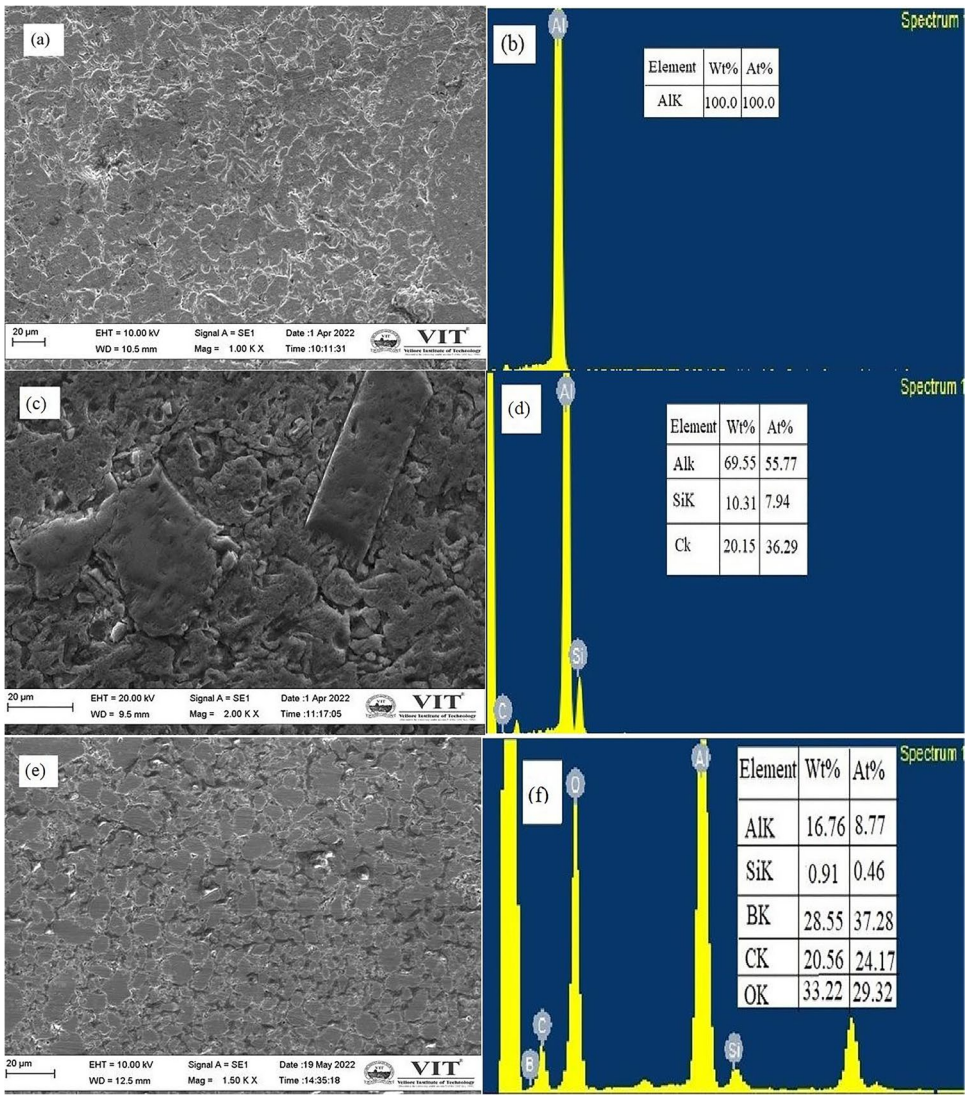

Fig. 3 (**a**) Microstructural image of pure aluminium matrix. (**b**) EDS analysis of pure aluminium matrix. (**c**) Microstructural image of Al+SiC composites. (**d**) EDS analysis of Al+3% SiC composite. (**e**) Microstructural images of Al+SiC+B_4C composite. (**f**) EDS analysis of Al+2%SiC+2% B_4C composite

LE was utilized. In this experiment, EN31 steel is used as a disc material, and the pin-shaped samples of aluminium matrix composites were obtained with the dimensions of 8 mm diameter and 12 mm length. All the wear test was performed with a sliding speed of 0.1 m/s over a sliding distance of 500 m for both applied load of 5 N and 10 N.

3 Results and Discussion

3.1 Surface Morphology Analysis

3.1.1 Aluminium Reinforced SiC Composite

Figure 4(a) shows pure aluminium with uniform fine-grain boundaries. Figure 4(b–d) shows SiC particles as uniformly distributed and embedded in the aluminium matrix. Homogenous distribution was seen in the SEM image throughout the Al matrix. Higher compacting load helped good interfacial bonding in the matrix and reinforcement particles. Higher sintering temperatures reduced the porosity level and improved the strength of the composites [19–22]. Figure 4(e, f) shows the agglomeration of particles found in samples with high reinforcement weight percentages. With the increase in the reinforcement ratio, increase in the aggregation of the particles was also seen. Variation in size was seen in the aluminium particles with typically spherical shapes, while the SiC particles generally has angular shapes and sharp corner edges.

3.1.2 Aluminium Reinforced Silicon Carbide and Boron Carbide

Figure 5(a) illustrates the micrograph of the Al+SiC+B_4C composite. The SEM micrograph revealed the presence of B_4C and SiC reinforcement in the aluminium matrix, shown in Fig. 5(b). Figure 5(c) shows the micrograph of the Al+SiC+B_4C composite. Homogenous distribution of the SiC and B_4C particles were seen in the Al matrix. The presence of intrinsic hard phases in B_4C reinforcement particles as well as the dispersion strengthening effects helped good bonding between the Al matrix and reinforcements. Figure 5(d, e) shows the agglomeration of particles formed in Al+5%SiC+2% B_4C and Al+6%SiC+2%B_4C composite samples. A significant improvement in agglomeration was seen with the addition of B_4C particles. During the sintering process, matrix and reinforcement phases were bounded by diffusion. The sintering temperature of 550°C softened the aluminium matrix and increased dislocation mobility, However, the strength of B_4C and elastic modulus remained unchanged [23, 24].

3.2 X-Ray Diffraction Analysis

3.2.1 Aluminium Reinforced SiC Composites

X-ray diffraction patterns of Al+SiC composites manufactured by the PM process are shown in Fig. 6(a). The high peaks (111), (200), (311) and (222) were obtained at 38.92°, 45.16°, 78.62° and 82.82° (2θ) for aluminium respectively.

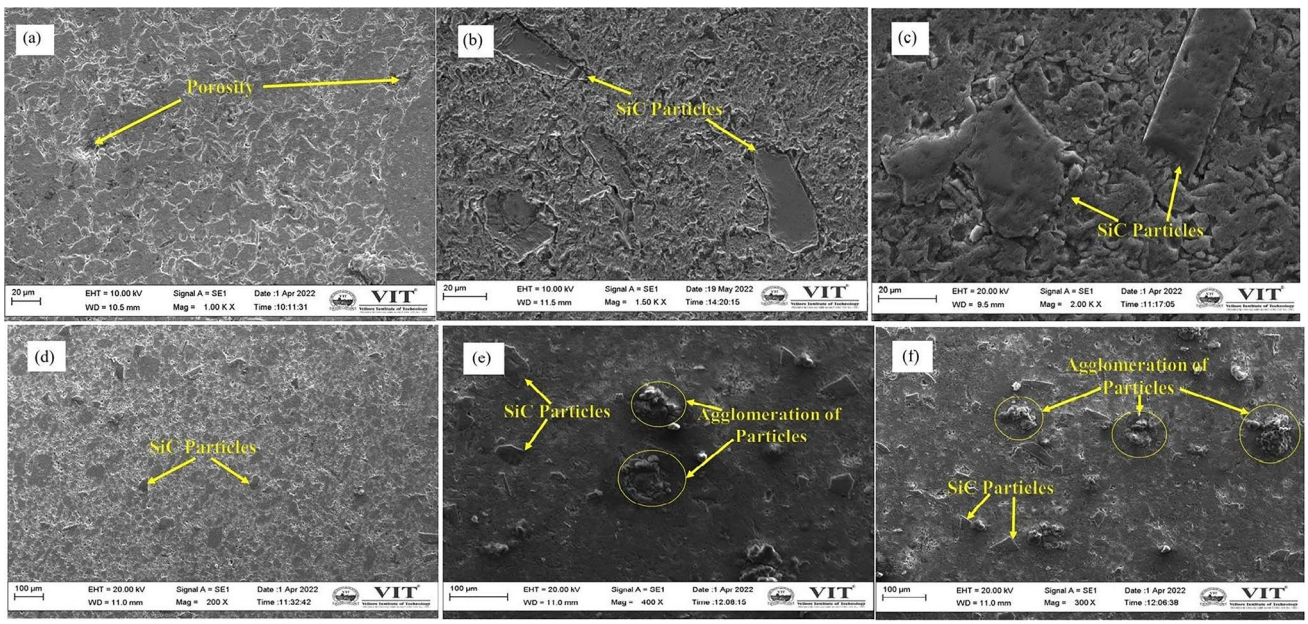

Fig. 4 Microstructure image of Al+SiC composite with different wt% of SiC (**a**) Pure aluminium (**b**) Al+2wt%SiC (**c**) Al+3wt%SiC (**d**) Al+4wt%SiC (**e**) Al+5wt%SiC (**f**) Al+6wt% SiC

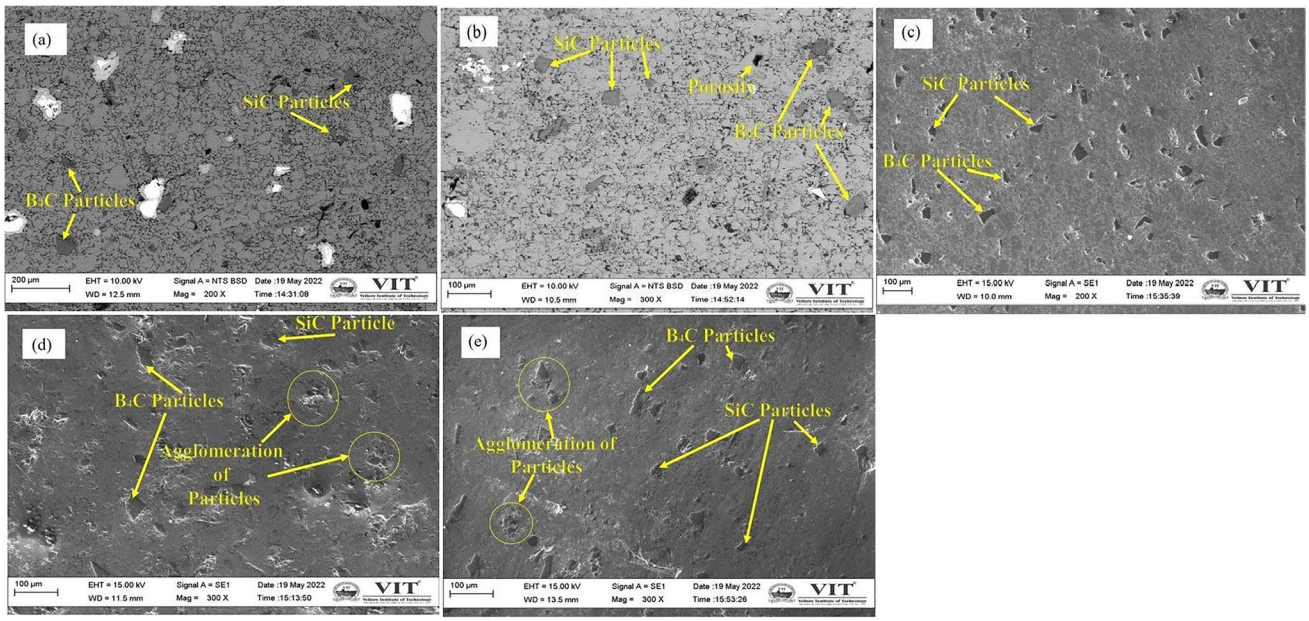

Fig. 5 Micrograph of Al+SiC+B_4C composites with different wt% of SiC and constant 2wt% of B_4C. (**a**) Al+2%SiC+2%B_4C (**b**) Al+3%SiC+2%B_4C (**c**) Al+4%SiC+2%B_4C (**d**) Al+5wt% SiC+2%B_4C (**e**) Al+6%SiC+2%B_4C

A weak peak (109) was obtained at (2θ) 65.51° for SiC. The average crystallite size of aluminium peaks ranged from 31.72 nm to 51.01 nm. Simultaneously, the average crystallite size of SiC peaks ranged from 35.10 nm to 36.00 nm. Al and SiC phases were observed in the phase analysis. As shown in Fig. 6(a) XRD graph, the intensity of SiC was low, due to reduced wt% of SiC in the Al matrix. A higher value of intensity value indicated the presence of atoms for a large number in a particular position. Al+SiC composite was seen with better uniform distribution of reinforcements [25, 26].

3.2.2 Aluminium Reinforced SiC and B_4C Composites

X-ray diffraction patterns of Al+SiC+B_4C composites manufactured with the use of the PM process are shown in Fig. 6(b). High peaks (111), (200), (311) and (222) were obtained at 38.33°, 44.60°, 78.10° and 82.28° (2θ) for aluminium respectively. The weak peaks (2θ) angle of 35.51°, 38.33° and 59.89° helped obtaining the miller indices planes of (102), (103) and (110) respectively for SiC. A small peak observed at a 2θ angle of 64.95° with miller indices of (018) confirmed the presence of B_4C. The average crystallite size of SiC peaks ranged from 33.10 nm to 34.00 nm. The average crystallite size of B_4C peaks ranged from 25.01 nm to 26.00 nm. Homogenous distribution of grain size was obtained in the Al+SiC+B_4C Composites. The XRD analysis revealed the absence of impurities and other peaks. The reinforcement B_4C has less intensity value and it is very difficult to identify the peak in the XRD pattern. Oxide peaks were not obtained in the XRD patterns, indicating the achievement of good composite samples through the use of the powder metallurgy process [27, 28].

3.3 Hardness Analysis

3.3.1 Aluminium Reinforced SiC Composite

The hardness values of Al+SiC composites are shown in Fig. 7(a). Hardness readings were taken at a distance of 0.5 mm in the cross-sectional layer. The hardness values of Aluminium reinforced SiC composites seen were higher than pure aluminium. An increase in the hardness value of the composites was seen following an increase in the SiC wt%. With the increase in SiC wt%, increase in the phase interface was also seen indicating improvement in the ability to withstand loading capacity, helping the increase in the hardness value of the composite [29]. Al-reinforced SiC (2 to 5 wt %) consistently improved the average hardness value from 39 to 42 HV. The hardness value of the Al composite (6 wt % SiC) achieved was 59 HV, which was 20.6% higher than that of the pure aluminium matrix (34 HV). The improvement of hardness had a big influence due to (a) grain refinement (b) resistance to dislocation movement and (c) solid dispersion. The use of the mechanical process helped reduction in grain size result increase deformation degree and exceptional distribution of the carbides [30, 31].

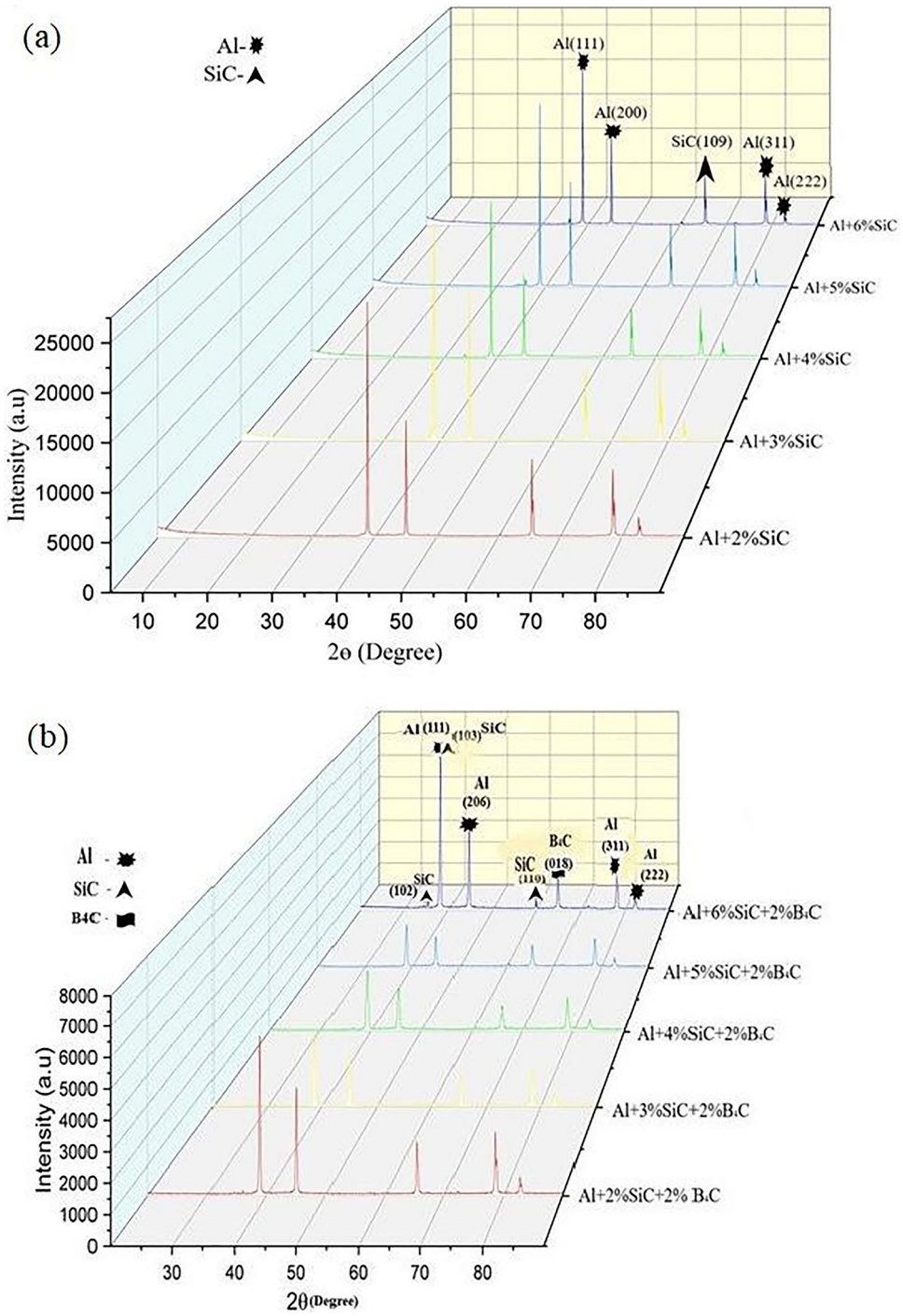

Fig. 6 (**a**) Phase analysis of Al+SiC composites. (**b**) Phase analysis of Al+SiC+B_4C composites

3.3.2 Aluminium Reinforced SiC and B_4C Composites

Hardness values shown in Fig. 7(b). indicate the addition of reinforcements such as SiC and B_4C to Al matrix alloy, helping improve considerably the hardness value due to the addition of stiffer and strong reinforcements. The composite hardness value of Al+4wt%SiC+2wt%B_4C achieved was 59 HV, which is 20.6% higher than the pure aluminium matrix (34 HV). The main improvement in mechanical properties was due to the B_4C particles, which served transfer of stress away from the aluminium matrix to the reinforcement particles. According to the orowan mechanism, the interaction between dislocation and particles was responsible for improved mechanical strength [20]. Al+5wt%SiC+2wt%B_4C and Al+6wt%SiC+2wt%B_4C composites had high agglomeration results as the influence of high porosity level, which caused a decrease in the hardness value of the composite. There was a decrease in the

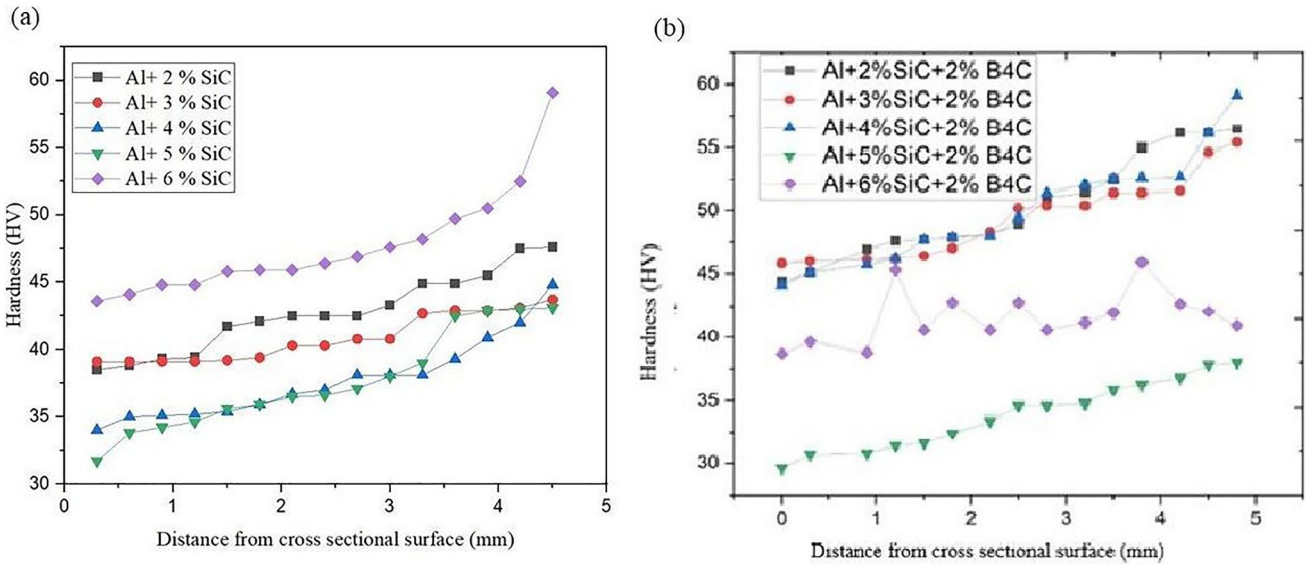

Fig. 7 (**a**) Cross-sectional hardness value of aluminium reinforced with different wt% of SiC composites. (**b**) Cross-sectional hardness value of aluminium reinforced with different wt % of SiC and constant wt % of B_4C composites

mechanical strength of the composite due to a mismatch between the shape and size of reinforcements and Al matrix particles [32, 33].

3.4 Compression Analysis

3.4.1 Aluminium Reinforced SiC Composites

Figure 8(a) shows the compression strength of aluminium strengthened with the use of silicon carbide particles. The addition of reinforcement in the form of hard ceramic particles led to an increase in the compression strength of aluminium matrix composites. The increasing weight (3 to 6) % of reinforcement particles in the matrix alloy showed the result as higher compressive strength. The addition of SiC, on the other hand, resulted in a greater compressive strength in comparison to monolithic alloy. The incorporation of more rigid reinforcement particles into the matrix alloy had the effect of creating impediments, which in turn inhibited the movement of dislocations and the plastic flow in the matrix. The limited material flow caused by the presence

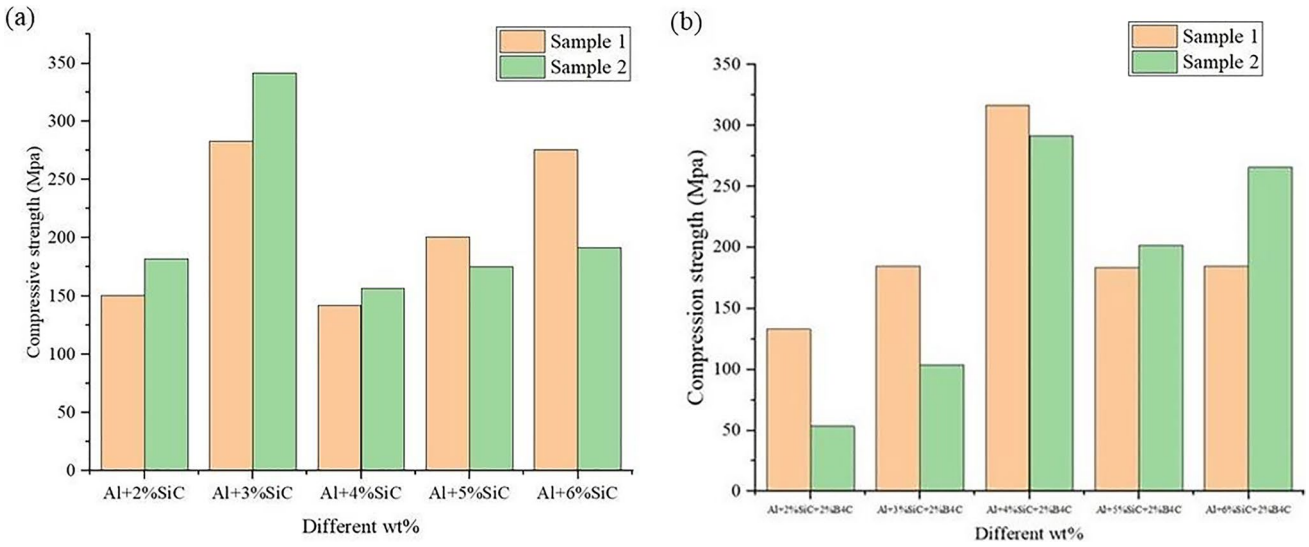

Fig. 8 (**a**) Compressive strength analysis of Al+SiC composites. (**b**) Compressive strength analysis of Al+SiC+B_4C composites

of reinforcing particles in aluminium composites, helped crack propagation leading to the formation of fracture can be slowed down, hence reducing the probability of the occurrence of fracture. In spite of this, the compressive strength of composites is significantly greater than that of pure aluminium. This can be attributed to the uniform distribution of reinforcement particles in aluminium composites and the presence of fewer residual pores, and grain refinement in the microstructure [34, 35].

3.4.2 Aluminium Reinforced SiC and B_4C Composites

The compression strength of reinforced hybrid aluminium with SiC and B_4C particles is depicted in Fig. 8(b). Compared to the pure aluminium, the composite material that contained reinforced B_4C particles exhibited a greater degree of compressibility. Increasing the weight (4 to 6) % of SiC and constant 2wt% of B_4C reinforcement particles in the matrix alloy showed higher compressive strength. Figure 8(b) shows the increase in compressive strength accomplished by the addition of wt% SiC and weight % of B_4C to the Al matrix. Another possible explanation for the increase in compressive strength of the composites is that the load bearing capabilities of carbides was higher, and as a result, the composite have better ability to withstand the compressive stresses [36].

3.5 Density Analysis

3.5.1 Aluminium Reinforced SiC Composites

Figure 9(a) shows a comparison between experimental density and theoretical density for Al/SiC composites. Theoretical calculation of the densities of AMC was made using the mixture rules

$$\text{Theoretical density} = (\rho \text{ of Al alloy} \times \text{wt\% of Al alloy}) + (\rho \text{ reinforcement} \times \text{wt\% of reinforcement}) \quad (1)$$

Experimental density was measured by Archimedes principle as per ASTM standard B962-15.

$$\rho_c = \frac{W}{W - W_1} \times \rho_w \quad (2)$$

ρ_w density of pure water

ρ_c density of Fabricated part

W Weight of composite in air

W_1 Weight of composite in water

$$\text{Relative density} = \text{Experimental density}/\text{Theoretical density} \times 100 \quad (3)$$

The relative density value of 92% obtained was the highest for the Al+6%SiC composite and the lowest relative density value of 90% was achieved for Al+3%SiC and Al+5%SiC composites, as shown in Fig. 9(b). The theoretical density values of the composite were slightly higher than the experimental density values of the composites. Voids constituted the major factor that had influence on the density of the composites [37, 38]. On the other hand, sintering time also has a significant impact on the density of the composites. Relative density was calculated using Eq. (3). Pure aluminium samples were tested for comparison purposes.

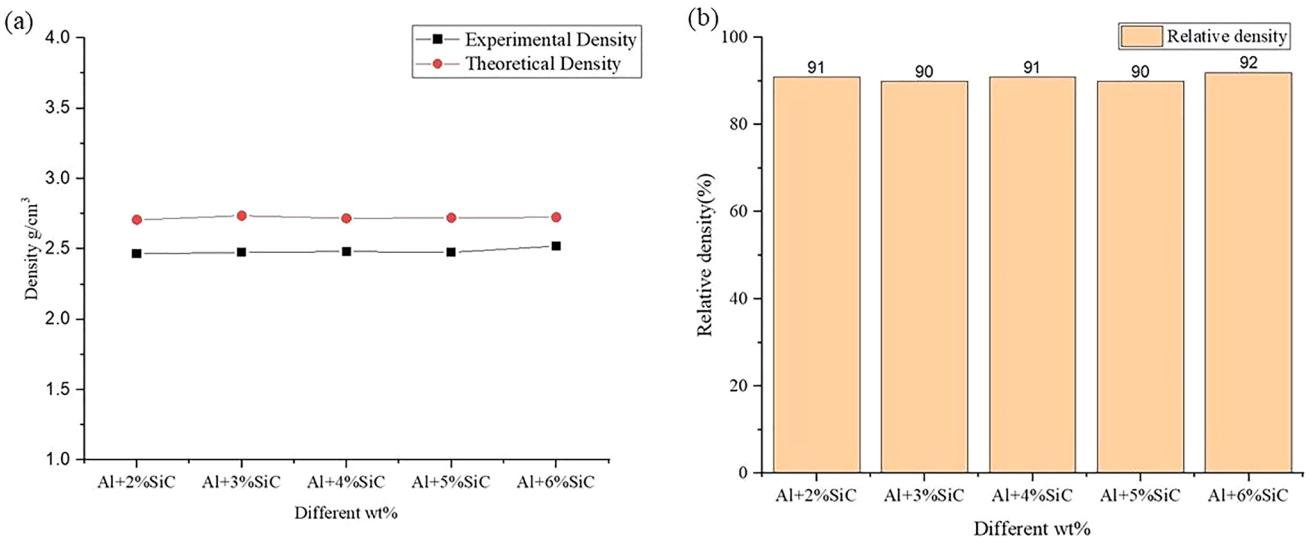

Fig. 9 (**a**) Density analysis of Al+SiC composites. (**b**) Relative Density analysis of Al+SiC composites

3.5.2 Aluminium Reinforced SiC and B_4C Composites

Figure 10(a) shows a comparison between the experimental density and theoretical density for Al+SiC+B_4C composites. The relative density value of 94% obtained was the highest Al+4%SiC+2%B_4C and the lowest relative density value of 80% was obtained for Al+5%SiC+2%B_4C composite, as shown in Fig. 10(b). The theoretical density values were slightly higher than those relating to the experimental density values. A reduction in the density of the composite was seen according to the form, size and wt% of reinforcement as well as the type of Al material used. An increase in reinforcement wt % was seen reducing the density value of the hybrid composites. The inclusion of B_4C particles in constant wt% caused an increase in the contact area of the particles. A mismatch in thermal coefficients between matrix alloy and B_4C reinforcement was seen during sintering affecting both surfaces, thereby helping the matrix-ceramic contact in the generation of the enormous quantity of dislocation density [39, 40].

3.6 Porosity

3.6.1 Aluminium Reinforced SiC Composites

The porosity of Sintered composites was calculated by using

$$\text{porosity } (\%) = \frac{\text{Theoretical density} - \text{Experimental density}}{\text{Theoretical density}} \times 100 \quad (4)$$

Optical Microscope images showed the presence of the lowest number of pores present in Al+6wt%SiC as shown in Fig. 11(a) and maximum number of pores present in Al+3wt%SiC composites as shown in Fig. 11(b). There was a slight decrease in the porosity values of the composites following an increase in the percentage of SiC particles as shown in Fig. 12(a). The porosity levels decrease, which results in an increase in the strength of the composite by effectively transferring load from matrix to reinforcement. Decreasing porosity levels can be attributed to the fact that grain growth and refinement was the major phenomenon that resulted in a good interface between matrix and reinforcement, which made the pores vanish. Additionally, by varying the compacting pressure at lower level the porosity is high, and at higher compacting pressure, the matrix material undergoes plastic deformation and enters in to the pores, which results the material with less porous. However, density is connected to porosity in some way. The percentage of porosity decreases whenever there is an increase in density. Due to the fact that sintering is a thermally activated process that is primarily controlled by diffusion, the temperature at which the samples were sintered had a significant impact on the degree to which the samples were compacted. Because of this, an increase in the sintering temperature results in an increase in the diffusion rate and a reduction in the number of pores in the bulk composite material. [41, 42].

3.6.2 Aluminium Reinforced SiC and B_4C Composites

Optical Microscope images indicated the presence of lowest number of pores are present in the Al+4wt%SiC+2wt%B_4C composite as shown in Fig. 11(c) and maximum number of pores in a hybrid composite of Al+5wt%SiC+2wt%B_4C as shown in Fig. 11(d). There was a rapid increase in the porosity values of the composites following an increase in the percentage of

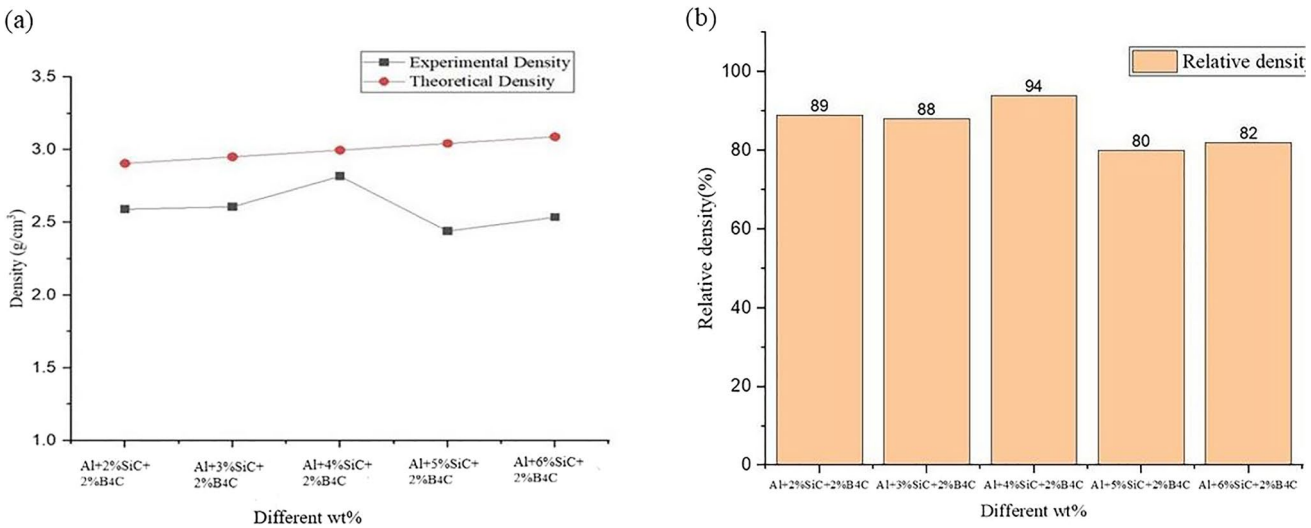

Fig. 10 (**a**) Density analysis of Al+SiC+B_4C composites. (**b**) Relative Density analysis of Al+SiC+B_4C composites

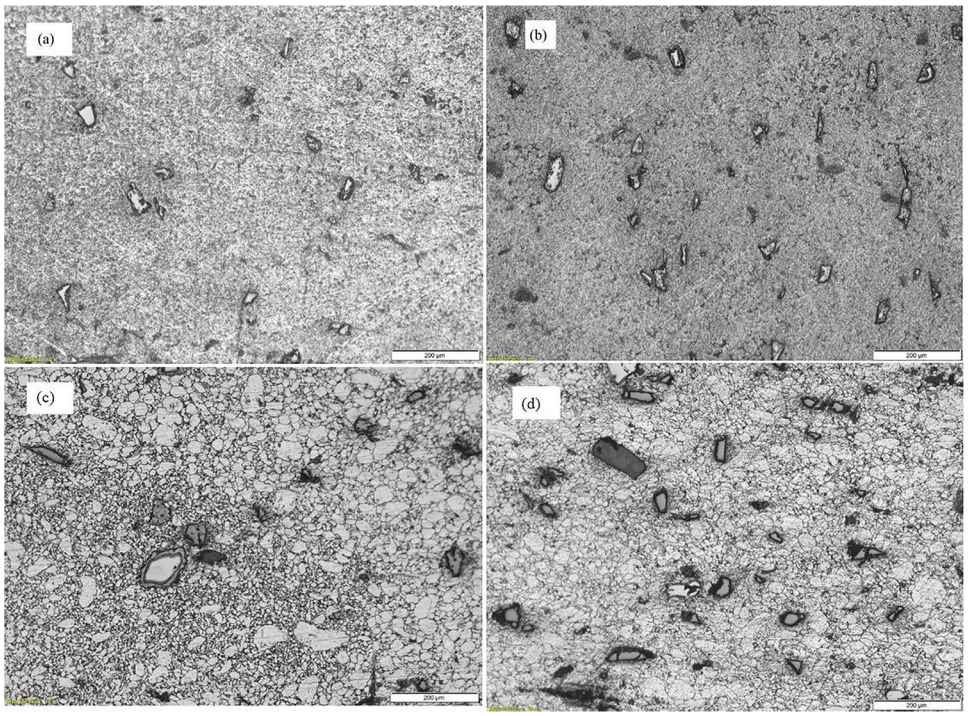

Fig. 11 Optical microscope images (**a**) Al+6wt%SiC composite (**b**) Al+3wt%SiC composite (**c**) Al+4wt%SiC+2wt%B_4C composite (**d**) Al+5wt% SiC+2wt%B_4C composite

SiC particles with constant B_4C particles as shown in Fig. 12(b). Poor wettability between the matrix and the particulates is the root cause for the increased porosity in the composites. The intrinsic properties of B_4C particles were harder than those of the matrix particles, and the development of some amount of particles clustering in high % content of reinforcement of composite. Hence, incompressible and high resistance seen during compaction, were found as causes of increasing the porosity level in the aluminium composites. It's possible that the irregular shape of the matrix material that was filled with reinforcement powders is the reason for the increase in porosity of the composites. Sintering time and temperature are of the utmost significance, when it comes to controlling densification and grain growth for the purpose of improving the mechanical properties of the composites [43, 44].

3.7 Wear Analysis

3.7.1 Aluminium Reinforced SiC Composites

The wear rates of pure aluminium and aluminium reinforced SiC composites were investigated with respect to the sliding distance by varying the applied loads as 5N and 10N. The wear test was carried out by two samples for each trial and the average value was determined and represented. Figure 13(a) and (b) shows the relationship between the wear rates and applied loads over a given sliding distance of 500 m for AMCs. An increased in the wear rates of AMCs was seen, When the applied load was raised from 5 to 10 N, a significant reduction in the wear rate of the composite material was seen, when compared to unreinforced aluminium. Continuous increased

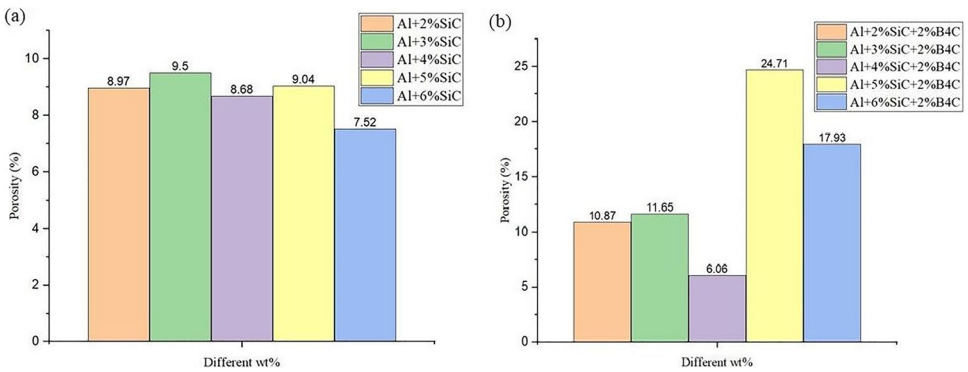

Fig. 12 Porosity values (**a**) Al+SiC composites (**b**) Al+SiC+B_4C composites

in the load on the aluminium pin, exhibited a continually increasing trend of wear due to direct metal to metal contact. Large-scale plastic deformation caused the generation of larger-sized wear debris on the occurrence of dry sliding. The composite, subjected to a given normal load, exhibited a slight increase in its wear rate. Aluminium–SiC composites exhibited significant plastic deformation, when tested with higher normal loads and sliding speeds. Deformation was seen due to plastic flow, related to instability of the aluminium matrix. When loading, with 10 N, more pull-out reinforcement particles were observed, indicating the occurrence of significant plastic deformation of the composite. The contribution of particles extracted to the formation of third body abrasion was also seen. The presence of ceramic particles in greater quantities in the tribo layer, was seen causing rupture. The virgin composite material is exposed in the contact zone, which leads to increased wear rate [45–48].

3.7.2 Effect of SiC Wt% on Coefficient of Friction

There are two factors that determine the coefficient of friction: the proportion of reinforcement wt% and the sliding distance as shown in Fig. 14(a) and (b). The SiC mass% in the material makes a direct contribution to an increase in the friction coefficient. A high surface roughness of the material is responsible for higher friction coefficient and its ability to separate tough SiC particles from Al-Matrix are responsible for higher friction coefficient. As the sliding distance increases, the surface area in contact with one another increases as well, leading to a higher friction coefficient.

3.7.3 Wear Mechanism of Al/SiC Composites

Figure 15(a) illustrates the typical wear pattern that occurred on the surface of aluminium matrix composites. When subjected to a load of 10 N, worn surfaces revealed that there

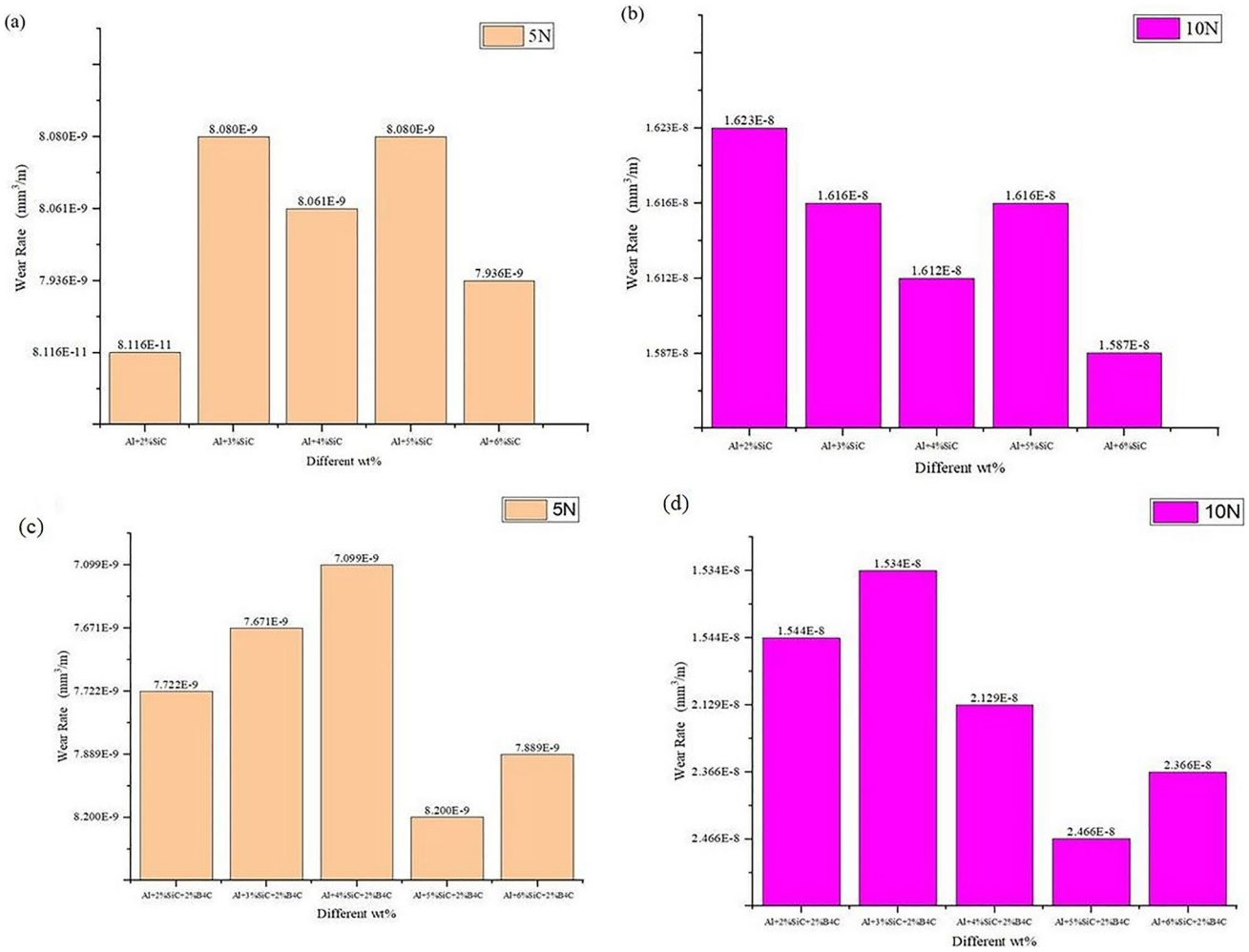

Fig. 13 Variation in wear rate of Al+SiC composites with respect to sliding distance of 500 m at a load of (**a**) 5N (**b**) 10N. Variation in wear rate of Al+SiC+B_4C composites with respect to sliding distance of 500 m at a load of (**c**) 5N (**d**) 10N

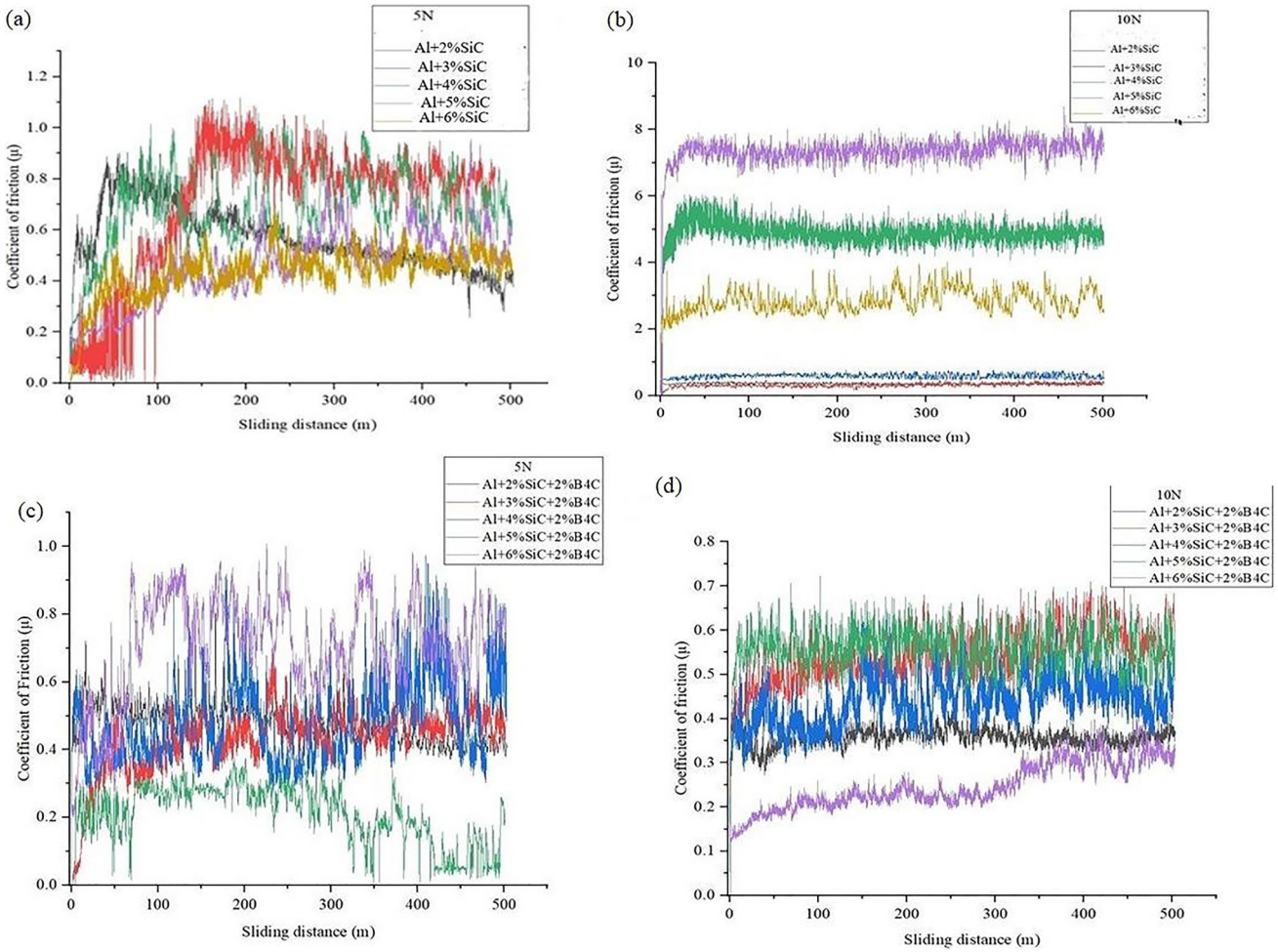

Fig. 14 Coefficient of friction versus sliding distance of Al+SiC composites (**a**) 5N (**b**) 10N. Coefficient of friction with sliding distance of Al+SiC+B_4C composites (**c**) 5N (**d**) 10N

was coverage of tribolayer and thin grooved lines at a speed of 0.1 m/s. A load range of 5 and 10 N and a speed range of 0.1 m/s have been shown to abrasion on aluminium hybrid composites. Figure 15(b) shows the presence of white particles of a significant number on the tribosurface, which may be present due to the oxidation on the surface that occurs as a result of frictional heating. During high loading and high velocity, delamination and a combination of abrasion, delamination, and adhesion were the most important mechanisms of wear.

3.7.4 Aluminium Reinforced SiC and B_4C Composites

Examination of the wear rates of pure aluminium and aluminium reinforced SiC+B_4C composites in with respect to the sliding distance was seen through variation in the applied load as 5N and 10N. The wear test was performed by two samples for each trial and the average value was calculated and represented. It was observed that the wear rate increases for hybrid composites with constant wt% of B_4C under all loading conditions as shown in Fig. 13(c) and (d). The following causes may be related to the increased wear rate with respect to applied load: rise in which temperature, plastic deformation and as a result, substantially increased wear rate occurs; which leads to adhesion wear. Increase in the wear rates of hybrid aluminium matrix composites was seen will increase in the sliding distance. A reduction was seen in the wear rate with increased wt% of SiC content with a constant applied load. The Archard's rule, which states that the hardness of composites is directly related to the amount of B_4C content, explained the reduction in wear rate of the composites. As a result, the rate of wear on composites was seen as inversely related to the hardness of the composites. In addition, the following facts contribute to the higher wear rates of the composites that occur with increased sliding distance. The friction force and wear rates were also affected by the wear debris that are formed during the sliding motion of aluminium matrix composites (pin) over counter disc materials (EN31 Steel). At constant load and uniform velocity,

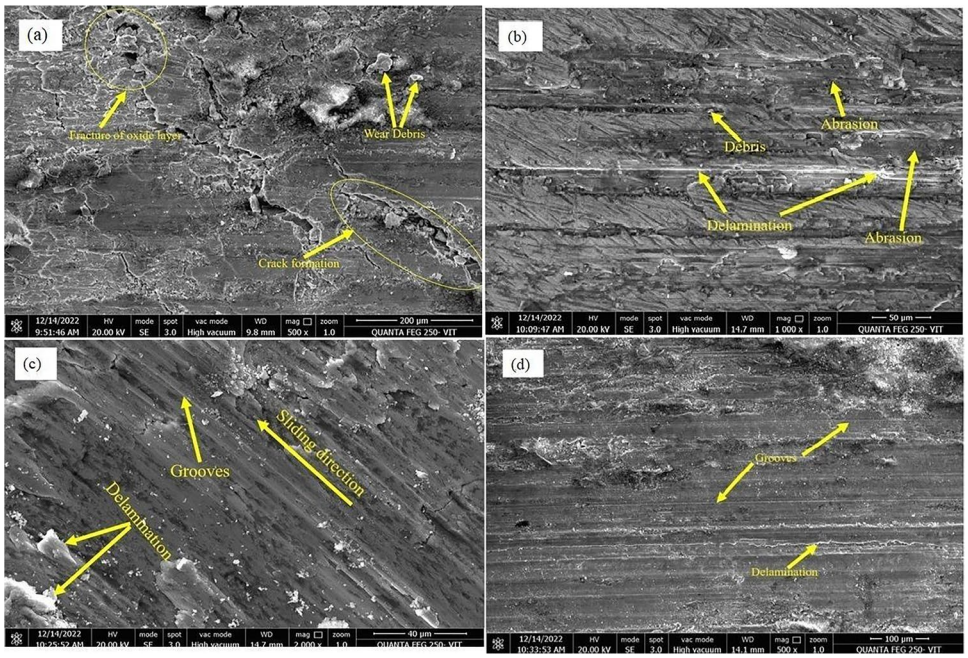

Fig. 15 FESEM showing worn out surface of (**a**) Al+2%SiC (**b**) Al+6%SiC (**c**) Al+3%SiC+2%B_4C (**d**) Al+5%SiC+2%B_4C

the increased amount of time that the surface of AMCs and counter material are in contact with one another increases, increases the activated thermal deformations [49–51].

3.7.5 Effect of SiC and B_4C Wt% on Coefficient of Friction

Determination of the coefficient of friction of both the unreinforced samples and the AMCs samples was done for the assessment of the wear behaviour of the samples. A decrease in the coefficient of friction that can be seen in Fig. 14(c) was caused by an increase in applied load. The coefficient of friction lowers with an increase in the wt% of SiC and B_4C particles, as seen in Fig. 14(d). The influence of B_4C on coefficient of friction is due to oxide layer. The B_4C particles are readily extracted and react with their surrounding environment, resulting in the formation of B_2O_3 oxide layer in the contact zone.

3.7.6 Wear Mechanism of Al/SiC/B_4C Composites

Occurrence of abrasion in Al+SiC+B_4C composite was seen as a result of the presence of dislodged and cracked SiC that got entrapped between the sliding surfaces or incorporated into soft aluminium matrix as shown in Fig. 15(c) and (d). The modulus of SiC particle was lower than that of B_4C reinforcement particle. The worn surfaces showed several plastically deformed grooves when subjected to 10 N and 0.1 m/s. Grooving and scratching played a more significant role in abrasive wear, when the loading condition and the rotational speed was higher. A subsurface fracture produced was the result of frequent repeated sliding behaviour, which led to the fatigue failure of the pin. There was increase in the cracks in the subsurface following an increase in travel distance and finally, shear deformation was developed on the surfaces. In addition, adhesion played most important role in causing plastic deformation, due to melting and thermal softening.

4 Conclusion

A comparison between aluminium matrix composites reinforced with different (2,3,4,5,6 wt %) of SiC particles were compared and hybrid composites of aluminium reinforced with different (2,3,4,5,6 wt %) of SiC was made and added with constantly 2wt% B_4C particles fabricated by powder metallurgy using the mechanical alloying process. A study of the microstructural characterization of the samples was made by Scanning electron microscope with EDS and X-ray diffraction methods. The experimental results indicated improvements in the hardness value of the composites caused by SiC reinforcement with aluminium matrix. A study of the mechanical behaviour of composites including the reinforcement effects on density and hardness was analysed. The observations were:

1. Microstructural analysis of Al+SiC reinforced composites revealed uniform distribution of SiC particles in the Al matrix. With the SiC wt% increased, there was also an increase in the phase interface also with the increase in the hardness value of the composite. Examination of the microstructure of Al+SiC reinforced composites, showed Al+4wt%SiC composite exhibiting homogenous distribution of the reinforcement in the matrix phase.

While Al+5wt% SiC and Al+6wt%SiC composites were found with agglomeration (cluster of particles).

Scanning electron microscope analysis revealed Al+4wt%SiC+2wt%B_4C hybrid composite getting a homogenous structure and strong interfacial bonding between matrix and reinforcement, whereas Al+5wt%SiC+2wt%B_4C and Al+6wt%SiC+2wt%B_4C composites had voids and agglomerations that increased with an increase in SiC reinforcements. Hence, there was a decrease in the mechanical strength of the composite due to a mismatch between the shape and size of the reinforcements and the Al matrix.

2. The XRD results of fabricated composites revealed the aluminium (111) phase getting high peak intensity, whereas Al (311), Al (222) phase got low-intensity peaks. XRD pattern exhibited the presence of B_4C and SiC high peaks with (018) and (103) planes respectively. While the phases of Al (311) and Al (222) got low-intensity peaks. No new compound was formed in the composites
3. Phase interface increased following an increase in SiC wt% and the high hardness value of 59 HV was obtained for the Al/6wt%SiC composite. Addition of B_4C, the Al+5wt%SiC+2wt%B_4C and Al+6wt%SiC+2wt%B_4C composites caused a reduction in the hardness value of 33 HV and 42 HV respectively, due to a mismatch between the shape and size of the reinforcement and Al matrix.
4. Composites with a higher compressive strength are Al+3%SiC and Al+6%SiC. The highest compression strength of reinforced hybrid aluminium composites is Al+4%SiC+2%B_4C. The addition of reinforcement in the form of hard ceramic particles led to an increase in the compression strength of aluminium matrix composites.
5. The high-density value of Al+6wt%SiC composite helped obtain 2.520 g/cm^3 due to a limited number of pores in the sample. A high density (2.817 g/cm^3) value was found in the Al+4wt%SiC+2wt%B_4C composite while the lower density (2.439 g/cm^3) was obtained in Al+5wt%SiC+2wt%B_4C composite. The addition of B_4C particles with higher reinforcement wt% (5 wt% and 6 wt%) of SiC caused a significant increase in the pores, thereby causing a decrease in the density value of the composites.
6. A lower wear rate was found in Al+2%SiC composites for 5N load and 500 m sliding distance. While the lower wear rate was found in Al+6%SiC composites for 10N load and 500 m sliding distance. The low wear rate was found to be Al+5%SiC+2%B_4C hybrid composites for both 5N and 10N loads and 500 m sliding distance. The B_4C reinforcement showed exceptional wear resistance and hardness qualities for hybrid AMCs. Addition of SiC wt%, decrease the coefficient of friction during the wear test. The coefficient of friction varies depending on the type of reinforcements and the matrix material.
7. Applications of a wide range find use in automobile and aerospace industries for AMC'S due to high wear resistance and mechanical properties. Al+SiC+B_4C hybrid composites can be replaced with Al+SiC composites for their better mechanical properties.
8. The applications of Al-Hybrid MMC exhibit extended mechanical and wear characteristics, and it can be recommended for different uses such as manufacturing of gears, drive shafts, brake drums, bearings, brake rotors, calipers and brake pad materials, etc.

4.1 Future Scope of Work

The future research will focus on different production techniques used for fabrication hybrid composites like equal channel angular pressing, friction stir process, and additive manufacturing in order to improve the mechanical performance of aluminium hybrid metal matrix composites. Various effects of reinforcements like CNT, graphene, Al_2O_3 and TiC on Al metal matrix composites can be studied for its mechanical characteristics.

Acknowledgements The authors would like to thank VIT University for providing the facilities for this research.

Authors' Contributions Mr. P Bharathi: designed the concept, interpreted the data and wrote the manuscript; Dr.T Sampath Kumar: analysed and revised the manuscript.

Funding The author(s) received no financial support for the research, authorship, and/or publication of this article.

Data Availability All data generated are analysed during this study are included in this published article.

Declarations

Ethics Approval Not applicable.

Consent to Participate Not applicable.

Consent for Publication The authors declare that the figures and tables used in this manuscript are original and are not published anywhere.

Competing Interests The authors declare no competing interests.

References

1. Suhael Ahmed S, Girisha HN (2020) Experimental investigations on mechanical properties of Al7075/TiB2/Gr hybrid composites. Mater Today Proc 46:6041–6044. https://doi.org/10.1016/j.matpr.2021.01.960
2. Srivyas PD, Charoo MS (2018) Role of fabrication route on the mechanical and tribological behavior of aluminum metal matrix composites - A review. Mater Today Proc 5:20054–20069. https://doi.org/10.1016/j.matpr.2018.06.372
3. Imran M, Khan ARA (2019) Characterization of Al-7075 metal matrix composites: A review. J Mater Res Technol 8:3347–3356. https://doi.org/10.1016/j.jmrt.2017.10.012

4. Bodukuri AK, Eswaraiah K, Rajendar K, Sampath V (2016) Fabrication of Al–SiC–B4C metal matrix composite by powder metallurgy technique and evaluating mechanical properties. Perspect Sci 8:428–431. https://doi.org/10.1016/j.pisc.2016.04.096
5. Arun Prakash J, Shanmughasundaram P (2017) Mechanical and tribological behaviour of aluminium metal matrix composites – an expatiate review. J Mines, Met Fuels 65:69–81
6. Borgonovo C, Apelian D (2011) Manufacture of aluminum nanocomposites: A critical review. Mater Sci Forum 678:1–22. https://doi.org/10.4028/MSF.678.1
7. Garg P, Jamwal A, Kumar D et al (2019) Advance research progresses in aluminium matrix composites: manufacturing & applications. J Mater Res Technol 8:4924–4939. https://doi.org/10.1016/j.jmrt.2019.06.028
8. Park J, Lee J, Jo I et al (2016) Surface modification effects of SiC tile on the wettability and interfacial bond strength of SiC tile/Al7075-SiCp hybrid composites. Surf Coatings Technol 307:399–406. https://doi.org/10.1016/j.surfcoat.2016.09.016
9. Nair SV, Tien JK, Bates RC (1985) Sic-reinforced aluminium metal matrix composites. Int Met Rev 30:275–290. https://doi.org/10.1179/imtr.1985.30.1.275
10. Halverson DC, Pyzik AJ, IiA A, Snowden WE (1989) Processing of boron carbide-aluminum composites. J Am Ceram Soc 72:775–780. https://doi.org/10.1111/j.1151-2916.1989.tb06216.x
11. Zhao N, Nash P, Yang X (2005) The effect of mechanical alloying on SiC distribution and the properties of 6061 aluminum composite. J Mater Process Technol 170:586–592. https://doi.org/10.1016/j.jmatprotec.2005.06.037
12. Singh J (2016) Fabrication characteristics and tribological behavior of Al/SiC/Gr hybrid aluminum matrix composites: A review. Friction 4:191–207. https://doi.org/10.1007/s40544-016-0116-8
13. Singh N, Mazumder R, Gupta P, Kumar D (2017) Ceramic matrix composites: Processing techniques and recent advancements. J Mater Environ Sci 8:1654–1660
14. Fenghong C, Chang C, Zhenyu W et al (2019) Effects of silicon carbide and tungsten carbide in aluminium metal matrix composites. SILICON 11:2625–2632. https://doi.org/10.1007/s12633-018-0051-6
15. Rahman MH, Al Rashed HMM (2014) Characterization of silicon carbide reinforced aluminum matrix Composites. Procedia Eng 90:103–109. https://doi.org/10.1016/j.proeng.2014.11.821
16. Fogagnolo JB, Velasco F, Robert MH, Torralba JM (2003) Effect of mechanical alloying on the morphology, microstructure and properties of aluminium matrix composite powders. Mater Sci Eng A 342:131–143. https://doi.org/10.1016/S0921-5093(02)00246-0
17. Liu J, Zhou B, Xu L et al (2020) Fabrication of SiC reinforced aluminium metal matrix composites through microwave sintering. Mater Res Express 7:125101–125108. https://doi.org/10.1088/2053-1591/abc8bf
18. Iqbal AKMA, Lim MJ, Nuruzzaman DM (2017) Effect of compaction load and sintering temperature on the mechanical properties of the Al-SiC nano-composite materials. AIP Conf Proc 1901:1–8. https://doi.org/10.1063/1.5010471
19. Oñoro J, Salvador MD, Cambronero LEG (2009) High-temperature mechanical properties of aluminium alloys reinforced with boron carbide particles. Mater Sci Eng A 499:421–426. https://doi.org/10.1016/j.msea.2008.09.013
20. Bhowmik A, Dey S, Dey D, Biswas A (2021) Dry sliding wear performance of Al7075/SiC composites by applying grey-fuzzy approach. SILICON 13:3665–3680. https://doi.org/10.1007/s12633-020-00930-3
21. Surya MS, Prasanthi G (2022) Effect of silicon carbide weight percentage and number of layers on microstructural and mechanical properties of Al7075/SiC functionally graded material. SILICON 14(4):1339–1348
22. Zhang L, Shi J, Shen C et al (2017) B4C-Al composites fabricated by the powder metallurgy process. Appl Sci 7:8–13. https://doi.org/10.3390/app7101009
23. Chand S, Chandrasekhar P, Roy S, Singh S (2021) Influence of dispersoid content on compressibility, sinterability and mechanical behaviour of B4C/BN reinforced Al6061 metal matrix hybrid composites fabricated via mechanical alloying. Met Mater Int 27:4841–4853. https://doi.org/10.1007/s12540-020-00739-0
24. Mohd Bilal Naim Shaikh SA and MAS (2018) Fabrication and characterization of aluminium hybrid composites reinforced with fly ash and silicon carbide through powder metallurgy. Mater Res Express 5:1-21.https://doi.org/10.1088/2053-1591/aab829
25. Abdizadeh H, Ashuri M, Moghadam PT et al (2011) Improvement in physical and mechanical properties of aluminum/zircon composites fabricated by powder metallurgy method. Mater Des 32:4417–4423. https://doi.org/10.1016/j.matdes.2011.03.071
26. Shin S, Lee D, Lee YH et al (2019) High temperature mechanical properties and wear performance of B4C/Al7075 metal matrix composites. Metals 9:1–11. https://doi.org/10.3390/met9101108
27. Soares E, Bouchonneau N, Alves E et al (2021) Microstructure and mechanical properties of AA7075 aluminum alloy fabricated by spark plasma sintering (SPS). Materials (Basel) 14:1–11. https://doi.org/10.3390/ma14020430
28. Suprapedi, Mulyadi, Sardjono P, Ramlan (2020) Preparation and characterization of alloy Al -SiC made by using powder metallurgy method. AIP Conf Proc 2221:5–11. https://doi.org/10.1063/5.0005086
29. Sankhla AM, Patel KM, Makhesana MA et al (2022) Effect of mixing method and particle size on hardness and compressive strength of aluminium based metal matrix composite prepared through powder metallurgy route. J Mater Res Technol 18:282–292. https://doi.org/10.1016/j.jmrt.2022.02.094
30. Canakci A, Varol T (2014) Microstructure and properties of AA7075/Al-SiC composites fabricated using powder metallurgy and hot pressing. Powder Technol 268:72–79. https://doi.org/10.1016/j.powtec.2014.08.016
31. Varol T, Canakci A (2013) Effect of weight percentage and particle size of B4C reinforcement on physical and mechanical properties of powder metallurgy Al2024-B4C composites. Met Mater Int 19:1227–1234. https://doi.org/10.1007/s12540-013-6014-y
32. Natrayan L, Santhosh MS, Mohanraj R, Hariharan R (2019) Mechanical and Tribological Behaviour of Al2O3&SiC Reinforced Aluminium Composites Fabricated via Powder Metallurgy. IOP Conf Ser Mater Sci Eng 561:1–7. https://doi.org/10.1088/1757-899X/561/1/012038
33. Akbarpour MR, Alipour S, Azar FL, Torknik FS (2016) Microstructure and hardness of Al-SiC nanocomposite fabricated through powder metallurgy method. Indian J Sci Technol 9:1–5. https://doi.org/10.17485/ijst/2016/v9i42/101515
34. Muraliraja R, Arunachalam R, Al-Fori I et al (2019) Development of alumina reinforced aluminum metal matrix composite with enhanced compressive strength through squeeze casting process. Proc Inst Mech Eng Part L J Mater Des Appl 233:307–314. https://doi.org/10.1177/1464420718809516
35. Narayanaswamy K, Praveen Kumar BS, Shivana S (2015) Development and Evaluation of Tensile and Compression Strength of Al based MMC. IJERT 3:1–3
36. Zhang J, Shi H, Cai M et al (2009) The dynamic properties of SiCp/Al composites fabricated by spark plasma sintering with powders prepared by mechanical alloying process. Mater Sci Eng A 527:218–224. https://doi.org/10.1016/j.msea.2009.08.067
37. Arora G, Sharma S (2019) Production of hybrid reinforcement by ball milling for development of aluminium matrix composites. World J Eng 16:357–362. https://doi.org/10.1108/WJE-10-2017-0338

38. Saxena A, Singh N, Kumar D, Gupta P (2017) Effect of ceramic reinforcement on the properties of metal matrix nanocomposites. Mater Today Proc 4:5561–5570. https://doi.org/10.1016/j.matpr.2017.06.013
39. Singh G, Goyal S (2018) Microstructure and mechanical behavior of AA6082-T6/SiC/B4C-based aluminum hybrid composites. Part Sci Technol 36:154–161. https://doi.org/10.1080/02726351.2016.1227410
40. Surya MS (2022) Effect of SiC weight percentage and sintering duration on microstructural and mechanical behaviour of Al6061/SiC composites produced by powder metallurgy technique. SILICON 14(6):2731–2739
41. Kumar K, Dabade BM, Wankhade LN (2021) Influence of B_4C and SiC particles on aluminium metal matrix composites: A brief overview. Mater Today Proc 44:2726–2734. https://doi.org/10.1016/j.matpr.2020.12.697
42. Bandil K, Vashisth H, Kumar S et al (2019) Microstructural, mechanical and corrosion behaviour of Al–Si alloy reinforced with SiC metal matrix composite. J Compos Mater 53:4215–4223. https://doi.org/10.1177/0021998319856679
43. El-Sayed Seleman MM, Ahmed MMZ, Ataya S (2018) Microstructure and mechanical properties of hot extruded 6016 aluminum alloy/graphite composites. J Mater Sci Technol 34:1580–1591. https://doi.org/10.1016/j.jmst.2018.03.004
44. Surya MS, Prasanthi G, Kumar AK, Sridhar VK, Gugulothu SK (2021) Optimization of tribological properties of powder metallurgy-processed Aluminum 7075/SiC composites using ANOVA and artificial neural networks. J Bio Tribo-Corros 7(4):1–12
45. Kumar GBV, Rao CSP, Selvaraj N (2012) Mechanical and dry sliding wear behavior of Al7075 alloy-reinforced with SiC particles. J Compos Mater 46:1201–1209. https://doi.org/10.1177/0021998311414948
46. Kumar A, Yeasin Arafath M, Gupta P et al (2020) Microstructural and mechano-tribological behavior of Al reinforced SiC-TiC hybrid metal matrix composite. Mater Today Proc 21:1417–1420. https://doi.org/10.1016/j.matpr.2019.08.186
47. Akbarpour MR, Alipour S (2018) Microstructure and tribological properties of nanostructured aluminum reinforced with SiC nanoparticles fabricated by powder metallurgy route. Trans Indian Inst Met 71:745–752. https://doi.org/10.1007/s12666-017-1207-6
48. Sridhar A, Lakshmi KP, Raju CH (2022) Microstructure, mechanical and tribological properties of Al7075/SiC/Graphite hybrid metal matrix composites. J Bio Tribo-Corros 8(3):1–15
49. Gupta P, Kumar D, Parkash O et al (2018) Dependence of wear behavior on sintering mechanism for Iron-Alumina Metal Matrix Nanocomposites. Mater Chem Phys 220:441–448. https://doi.org/10.1016/j.matchemphys.2018.08.079
50. Uthayakumar M, Aravindan S, Rajkumar K (2013) Wear performance of Al-SiC-B4C hybrid composites under dry sliding conditions. Mater Des 47:456–464. https://doi.org/10.1016/j.matdes.2012.11.0
51. Sharifi EM, Karimzadeh F (2011) Wear behavior of aluminum matrix hybrid nanocomposites fabricated by powder metallurgy. Wear 271:1072–1079. https://doi.org/10.1016/j.wear.2011.05.015